ICIC Express Letters
Volume **19**, Number **6**, June **2025**

ICIC International ©2025 ISSN 1881-803X
pp. **677–684**

A STUDY ON THE ANALYSIS AND CLASSIFICATION OF GAIT STATES USING KEYPOINT INFORMATION

Ryusei Tanno, Thi Thi Zin* and Cho Nilar Phyo

Graduate School of Engineering
University of Miyazaki
1-1, Gakuen kibanadai-Nishi, Miyazaki 889-2192, Japan
hl19033@student.miyazaki-u.ac.jp; chonilar@cc.miyazaki-u.ac.jp
*Corresponding author: thithi@cc.miyazaki-u.ac.jp

Received September 2024; accepted November 2024

Abstract. *In Japan, 29.0% of the population is elderly, and as this demographic grows, the need for care increases, straining healthcare facilities. Mobility issues, especially falls, significantly contribute to this demand. This study aims to provide a non-contact, accessible method for quantifying gait states in elderly individuals using image processing technology. The experiment, conducted at a commercial facility in Higashi-Osaka City, involved capturing walking sequences from two viewpoints with RGB cameras. Using OpenPose to extract skeletal keypoints, walking balance and kyphosis were evaluated. The angle between the neck and hips served as an indicator for balance, classified as "Normal", "Warning", or "Danger", while kyphosis was classified as "Normal", "Mild", or "Severe". Results showed a correlation between age and balance decline, with older individuals having more "Danger" classifications. Kyphosis was also accurately identified through visual posture comparison.*
Keywords: Image processing, OpenPose, Elderly people, Gait balance, Kyphosis

1. Introduction.

1.1. Background.

As of October 1, 2022, Japan's total population was 124.95 million, with 36.24 million people aged 65 and over, representing 29.0% and indicating a high aging rate. This includes 16.87 million early elderly (aged 65-74) and 19.36 million late elderly (aged 75 and over), with the latter group's proportion rising [1]. Figure 1 shows the elderly population trend from 1950 to 2070, indicating a continuous aging rate increase.

Additionally, the number of people needing care has grown with the aging population. Figure 2 shows that certified care recipients increased from 2.47 million in 2000 to 6.69 million in 2020, a 2.7-fold rise. Walking-related issues like falls, fractures, joint diseases, and frailty account for 36% of these cases [2].

Additionally, gait disorders are common in elderly populations and their prevalence increases with age. At the age of 60 years, 85% of people have a normal gait, but at the age of 85 years or older, this proportion has dropped to 18% [3,4]. The following characteristics are observed in elderly walking patterns [5]:

- Decrease in walking speed;
- Decrease in step length;
- Reduction in walking rate (number of steps taken in a certain period);
- Forward tilt of the trunk, kyphosis;
- Reduction in the range of motion of the hip, knee, and ankle joints;
- Decrease in muscle strength, making it difficult to lift the feet;
- Decrease in lower limb support time (time during which the sole of the foot is on the ground supporting the body).

DOI: 10.24507/icicel.19.06.677

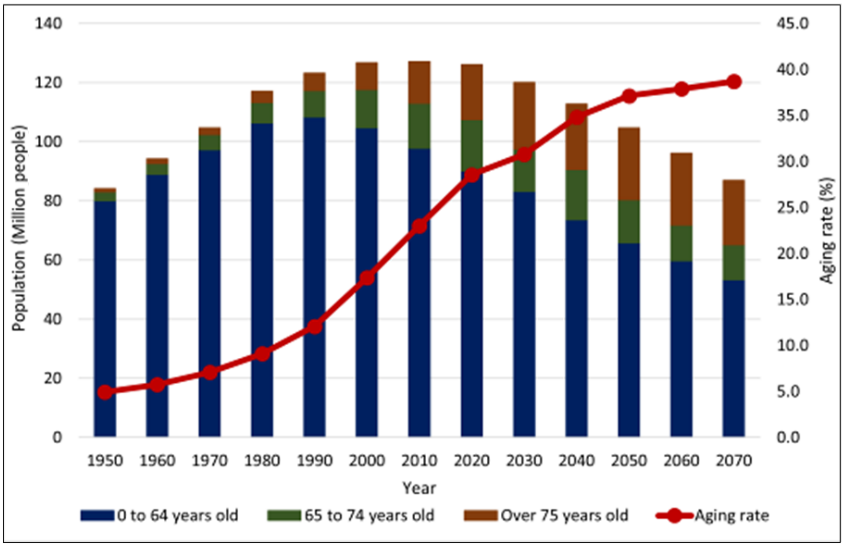

FIGURE 1. Trends in the elderly population in Japan (color online)

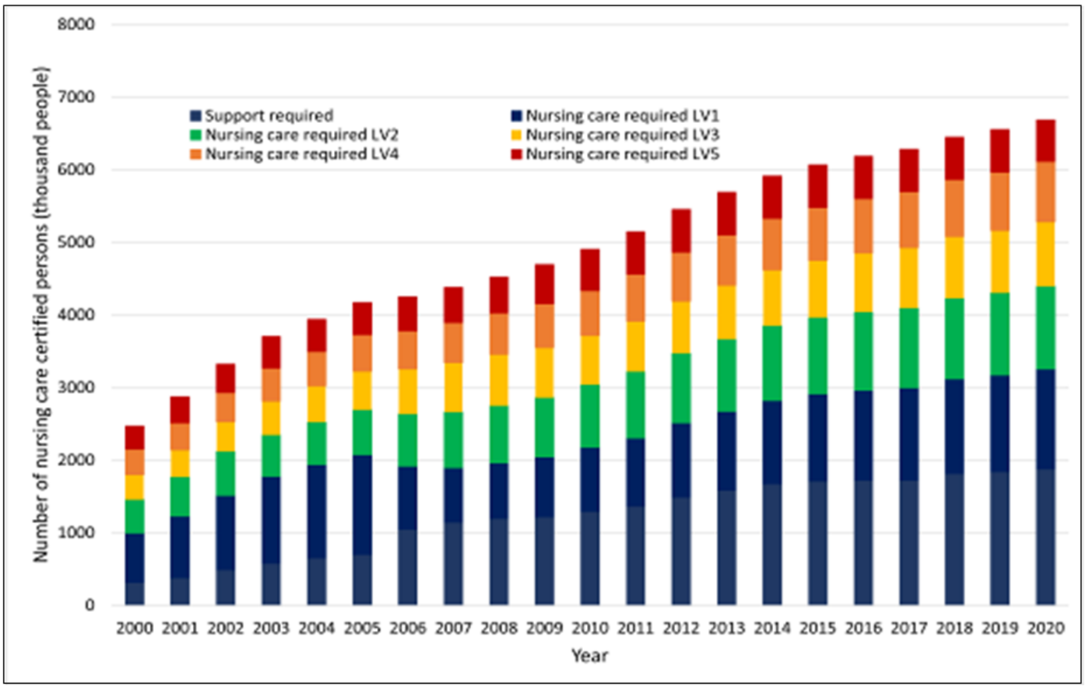

FIGURE 2. Trends in the number of certified recipients (color online)

Walking is a crucial function in daily living activities, and a decline in walking ability leads to a decrease in the level of activities of daily living (ADL). Among walking abilities, walking speed is particularly strongly associated with mortality risk and is considered an indicator of physical and daily life functions in the elderly. Walking speed gradually decreases after the age of 65, and it is said that after the age of 80 for men and 75 for women, it begins to interfere with daily life. Women experience a decline in walking ability five years earlier than men, accompanied by a decrease in daily living functions. This decline is related not only to muscle weakness and reduced balance due to aging but also to the increased risk of cerebrovascular disease, Parkinson's disease, cardiovascular disease, and musculoskeletal disorders in the elderly [6,7].

1.2. **Research objectives.** As stated in Section 1.1, Japan's aging population is leading to an increase in individuals certified as requiring long-term care. However, the number of healthcare and caregiving professionals remains nearly unchanged, resulting in a serious labor shortage. Extending healthy life expectancy, defined as the period during which individuals live without restrictions on daily activities due to health issues [8], has been proposed as a solution. Falls and fractures are primary triggers that shift healthy elderly individuals into a state of needing care, with falls being closely related to walking ability.

This study aims to contribute to addressing labor shortages in the healthcare and caregiving sectors by developing new indicators to quantify elderly individuals' walking states using image processing technology. This research proposes a method that uses only non-contact, non-invasive RGB cameras, allowing for broad application across various environments. In comparison to related research by Benenaula et al. [9], which used CNN and SVM to classify normal, hemiparetic, and paraparetic gaits, this study focuses on analyzing walking speed, balance, and their association with activities of daily living (ADL) and mortality risk. This approach is expected to make significant contributions to preventive healthcare.

The paper is organized as follows: Section 2 describes the experimental environment, methods, and the proposed approach; Section 3 presents the results; and Section 4 summarizes conclusions and future directions.

2. Method.

2.1. Experiment environment. The capturing was conducted at a commercial facility in Higashi-Osaka City, Osaka Prefecture, Japan. Two RGB cameras were installed at a height of 2.85 meters as shown in Figure 3. The cameras were set to a resolution of 1920 × 1080 and a frame rate of 30 fps. The walking section was set to 6.3 meters, capturing a round trip of 12.6 meters.

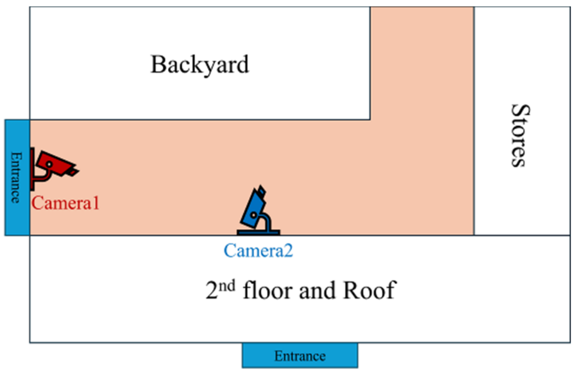

(a) Overhead diagram of the capturing environment

(b) Actual camera setup

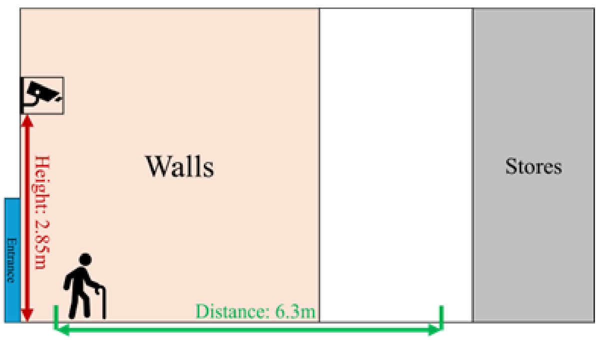

(c) Cross-sectional diagram of the capturing environment

FIGURE 3. Schematic diagram of the capturing environment

(a) The images obtained from Camera 1 (b) The images obtained from Camera 2

FIGURE 4. Examples of the images that can be obtained

Camera 1 in Figure 3 captured the walking from the front as depicted in Figure 4(a), while Camera 2 captured it from the side as shown in Figure 4(b).

2.2. **Method outline.** This study proposes a method for real-time detection of posture during walking (anterior-posterior and lateral balance). Unlike previous studies that relied on 3D sensors or accelerometers, this method utilizes a simple system based on RGB cameras and OpenPose, making it broadly accessible and applicable.

The overall flowchart of the proposed method is shown in Figure 5. Key point information, obtained in advance, is input, and tracking is conducted for each target object. Following tracking, for the data obtained from the camera, the angle between the neck key point and hip key point is calculated and used as an indicator.

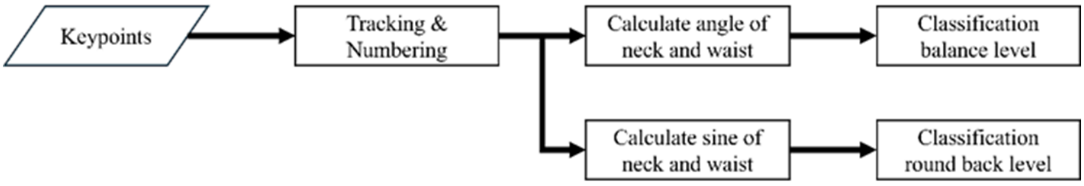

FIGURE 5. Overall flowchart

2.3. **Key point detection.** The key points are obtained using OpenPose [10]. The key points acquired in this study consist of 25 points, as shown in Figure 6.

2.4. **Tracking process.** In this study, as mentioned in Section 2.1, the filming environment is a commercial facility. Therefore, the key points obtained include data from an unspecified number of individuals. To extract data for each person, tracking processing was performed.

In the tracking process, attention was focused on the key point of the hip (point with index 8 in Figure 6). The tracking process follows the flow shown in Figure 7. The coordinates of the hip key point obtained in the first frame are stored. Next, the hip key point is obtained in the second frame, and the Euclidean distance between these two points is calculated. The threshold for the Euclidean distance is set to 20. If the calculated Euclidean distance is within the threshold, the points are considered to belong to the same person; if it exceeds the threshold, the points are classified as belonging to a new person, and an ID is assigned. The processing is then carried out for each ID.

2.5. **Feature extraction.** The processing of the data obtained from Camera 1 is described as follows. Focusing on the key points of the Hip (point with index 8 in Figure 6) and the neck (point with index 1 in Figure 6), the angle between these two points is

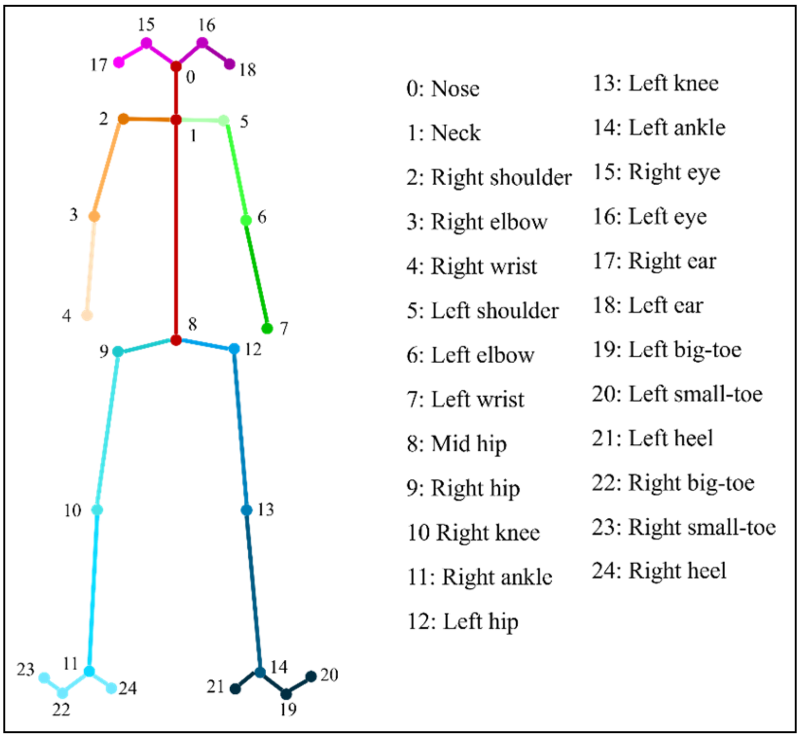

FIGURE 6. OpenPose 25 key points

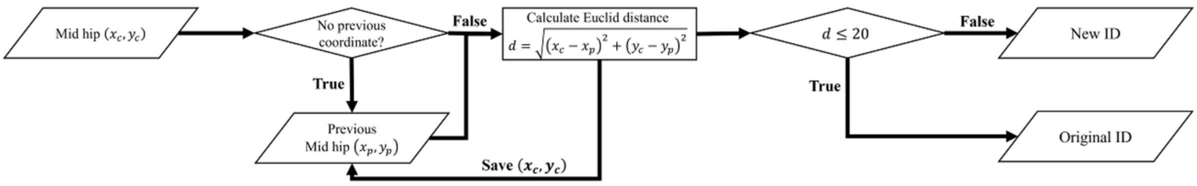

FIGURE 7. Tracking flowchart

calculated. The calculation of the angle is done using the arctangent of the neck (x_{11}, y_{11}) and hip (x_{81}, y_{81}) points as shown in Equation (1).

$$\theta = \tan^{-1}(x_{11} - x_{81}/y_{11} - y_{81}) \tag{1}$$

After calculating the angle, it is classified as follows based on 90 degrees, as shown in Table 1: if the absolute value is within 5 degrees, it is considered Normal; if the absolute value is greater than 5 degrees but within 10 degrees, it is considered Warning; and if the absolute value exceeds 10 degrees, it is considered Danger.

TABLE 1. Legend for classification by angle

Degree range	**Classification**
$85° \leq \theta \leq 95°$	Normal
$80° \leq \theta < 85°$ or $95° < \theta \leq 100°$	Warning
$\theta < 80°$ or $\theta > 100°$	Danger

Additionally, for the data obtained from Camera 2, the angle between the neck (x_{12}, y_{12}) and hip (x_{82}, y_{82}) key points is calculated. From the calculated angle, the sine value is derived and used as an indicator. Using 1.00 as the baseline for the sine value, the classifications are as follows: 0.96 to 1.00 is considered normal, 0.86 to 0.96 is considered mild kyphosis [11], and below 0.86 is considered severe kyphosis. The classification legend is summarized in Table 2.

Table 2. Legend for classification sine value

Sine range	Classification
$0.96 \leq \sin\theta \leq 1.00$	Normal
$0.86 \leq \sin\theta < 0.96$	Mild kyphosis
$\sin\theta < 0.86$	Severe kyphosis

3. **Result.** First, the data acquisition method is described.

As mentioned in Section 2.1, data acquisition involves walking 12.6 meters back and forth. Data was collected under three walking patterns: normal walking, deliberately walking energetically, and deliberately walking poorly. The processing was performed on data filmed in April 2023, and the effectiveness of the proposed indicators was evaluated.

For the indicators representing the upper body, the proportion of each classification – Normal, Warning, and Danger – calculated according to Table 1, is used as an indicator. This proportion is determined by dividing the number of frames classified as Normal, Warning, and Danger by the total number of frames in the sequence. Table 3 summarizes the global ID, age, walking classification (N: Normal for walking, H: Healthy action for walking, and UH: Unhealthy action for walking), total number of frames in the sequence, and the counts and proportions of frames classified as Normal, Warning, and Danger.

Table 3. Result of gait balance indicator

ID	Age	Walking class	Total frames	Normal frames	Normal rate [%]	Warning frames	Warning rate [%]	Danger frames	Danger rate [%]
12	83	N	403	359	89.1	41	10.2	3	0.744
		H	303	275	82.6	46	13.8	12	3.60
		UH	339	291	85.8	46	13.6	2	0.590
11	66	N	328	324	98.8	4	1.22	0	0
		H	439	419	95.4	20	4.56	0	0
		UH	393	375	95.4	18	4.58	0	0
22	83	N	418	370	88.5	46	11.0	2	0.478
		H	494	408	82.6	80	16.2	6	1.21
		UH	642	531	82.7	102	15.9	9	1.40
27	83	N	520	473	91.0	30	5.77	17	3.27
		H	489	462	94.5	25	5.11	2	0.409
		UH	411	328	79.8	62	15.1	21	5.11
30	72	N	301	187	62.1	58	19.3	56	18.6
		H	345	199	57.9	121	35.1	25	7.25
		UH	351	232	66.4	72	17.9	2	0.570

Furthermore, a subset of the data from Table 1 is extracted, and the angle transitions are illustrated in a graph in Figure 8.

Next, the sine values corresponding to each ID are summarized in Table 4. The sine values are extracted when the body is at or closest to the center of the camera's field of view. Since two values are extracted in one walking sequence, their average is calculated and used as the indicator. The obtained values are then classified based on the range of Sine listed in Table 2, which is used to determine the degree of forward tilt of the upper body.

4. **Conclusion.** In this paper, we developed indicators to visualize the walking state of elderly individuals using image processing techniques. From Camera 1 data, we created an indicator for left-right balance during walking, and from Camera 2 data, we developed an indicator for kyphosis during walking.

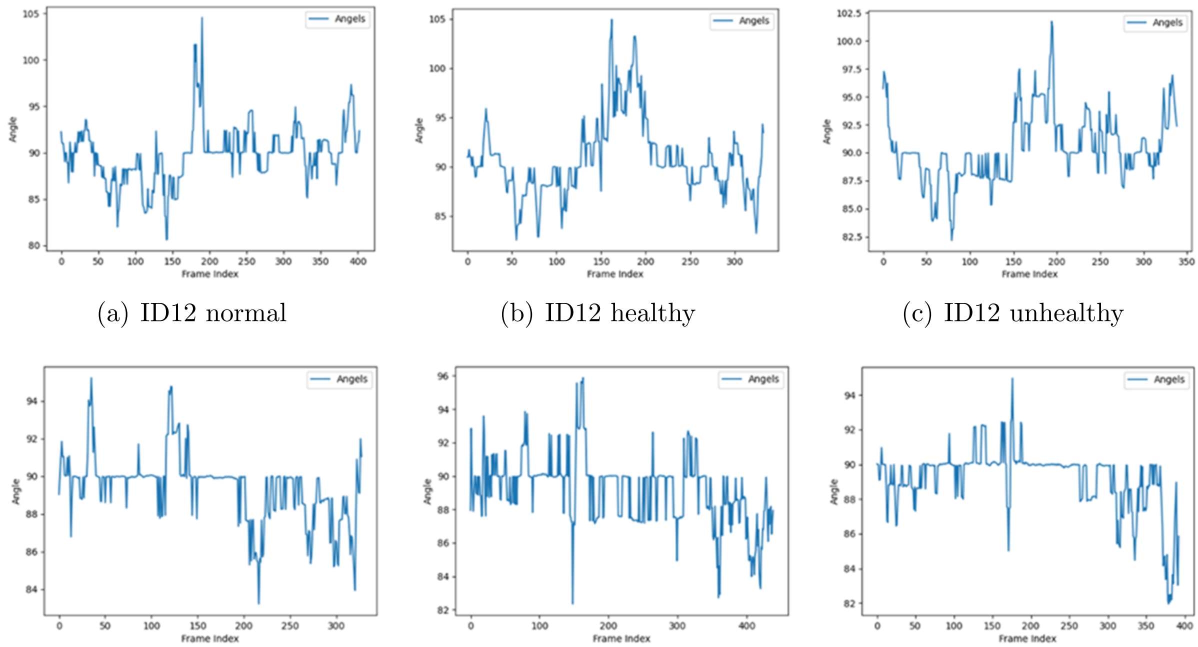

(a) ID12 normal (b) ID12 healthy (c) ID12 unhealthy

(d) ID11 normal (e) ID11 healthy (f) ID11 unhealthy

Figure 8. Transitions of trunk angle

Table 4. Result of kyphosis indicator

ID	Age	Walking class	Sine	Classification
12	83	N	0.974	Normal
		H	0.997	Normal
		UH	0.990	Normal
11	66	N	0.989	Normal
		H	0.991	Normal
		UH	0.997	Normal
22	83	N	0.952	Mild kyphosis
		H	0.946	Mild kyphosis
		UH	0.913	Mild kyphosis
27	83	N	0.994	Normal
		H	0.970	Normal
		UH	0.994	Normal
30	72	N	0.978	Normal
		H	0.974	Normal
		UH	0.986	Normal

First, regarding balance during walking, we observed a correlation with age. ID12 is a healthy 83-year-old male, and ID11 is a healthy 66-year-old male. However, ID11 had zero Danger classifications, suggesting that this indicator can reflect the decline in balance ability with age. On the other hand, balance transitions due to movements to avoid obstacles were also classified as abnormal. Therefore, it is necessary to distinguish whether a balance disruption is due to a loss of balance or an attempt to avoid an obstacle, based on the relationship between frames.

Next, regarding the degree of kyphosis, individuals who exhibited kyphosis were correctly classified. Figure 9 shows silhouette images. (a) is ID22, classified as having mild kyphosis, while (b) and (c) are ID12 and ID27, respectively, both same age. Comparing

(a) ID22 silhouette (b) ID12 silhouette (c) ID27 silhouette

FIGURE 9. Silhouette images

these, the image in (a) shows a curved back, while (b) and (c) do not appear as curved, indicating that the degree of kyphosis was correctly detected.

Finally, our prospects include further processing on more data to confirm the effectiveness of the indicators, beyond the data from April 2023. Additionally, although not implemented in this study, we aim to develop indicators for features directly related to walking, such as stride length, gait cycle, and walking speed. Ultimately, we intend to implement a system that comprehensively quantifies the walking state using all indicators, allowing for classification and temporal comparison of walking states.

REFERENCES

[1] Japan Cabinet Office, 2023, *Annual Report on the Aging Society: 2023*, https://www8.cao.go.jp/kourei/whitepaper/w-2023/html/zenbun/index.html, Accessed on May 19, 2024 (in Japanese).
[2] Japan Cabinet Office, 2019, *Annual Report on the Aging Society: 2019*, https://www8.cao.go.jp/kourei/whitepaper/w-2019/html/zenbun/index.html, Accessed on May 19, 2024 (in Japanese).
[3] B. R. Bloem, J. Haan, A. M. Lagaay, W. van Beek, A. R. Wintzen and R. A. Roos, Investigation of gait in elderly subjects over 88 years of ago, *Journal of Geriatric Psychiatry and Neurology*, vol.5, no.2, pp.78-84, 1992.
[4] L. Sudarsky, Gait disorders: Prevalence, morbidity, and etiology, *Adv. Neurol.*, vol.87, pp.111-117, 2001.
[5] Kenko Choju Net, 2023, *Relationship between Gait Ability and Diseases in the Elderly*, https://www.tyojyu.or.jp/net/kenkou-tyoju/undou-kiso/hokou.html, Accessed on May 19, 2024 (in Japanese).
[6] Japan Cabinet Office, *Materials Submitted by the Committee Regarding the Next National Health Promotion Campaign*, 2012, http://www.mhlw.go.jp/stf/shingi/2r9852000001zz5s-att/2r9852000001zz79.pdf, Accessed on June 19, 2024 (in Japanese).
[7] H. Maruyama, Physical function and walking in elderly individuals, *Physical Therapy Science*, vol.14, no.3, pp.102-105, 1998 (in Japanese).
[8] T. Sato, Average life expectancy and healthy life expectancy, *e-Healthnet*, Ministry of Health, Labour and Welfare, 2022, https://www.e-healthnet.mhlw.go.jp/information/hale/h-01-002.html, Accessed on May 27, 2024 (in Japanese).
[9] S. Benenaula, M. D. Trelles, L. E. Garza-Castañón and L. I. Minchala, Classification of gait anomalies by using space-time parameters obtained with pose estimation, *International Journal of Innovative Computing, Information and Control*, vol.18, no.6, pp.1913-1927, DOI: 10.24507/ijicic.18.06.1913, 2022.
[10] Z. Cao, G. Hidalgo, T. Simon, S.-E. Wei and Y. Sheikh, OpenPose: Realtime multi-person 2D pose estimation using part affinity fields, *IEEE Transactions on Pattern Analysis and Machine Intelligence*, 2019.
[11] S. Fukuda, *[Expert Explanation] The Dangers of Ignoring Kyphosis: 8 Exercises to Prevent and Improve a Rounded Back*, LIFULL Nursing Care, https://kaigo.homes.co.jp/manual/healthcare/kaigoyobo/shisei/, Accessed on June 19, 2024 (in Japanese).